



Production of silver nanoparticles from *Catharanthus roseus* under controlled physiological environment: A pioneer advancement to combat antibiotic-resistant microbes

Monika Gupta^{1*}

¹Amity Institute of Biotechnology, Amity University Madhya Pradesh, Maharajpura road, Gwalior (MP)-474005, India

*Corresponding author email: biotech.monikaphd@gmail.com

ABSTRACT

The present research work focuses on synthesis of silver nanoparticles from callus extract prepared from leaf explants of *in vitro* grown *C. roseus* under controlled conditions. The secondary metabolites present in *C. roseus* (an important medicinal plant) act as reducing and capping agents by which size of nanoparticles can be regulated. Regulation of shape and size of nanoparticles by physiological factors was not studied extensively till date under *in-vitro* conditions. The present study aims to discover cost-efficient, highly feasible, less time consuming and greener methods to produce nanoparticles. The callus culture was exposed to varying photoperiods (16/8 hours light and dark: controlled, 16/8 hours dark/light: short days, 20/4 hours light/dark: long days). In another experiment, pH was altered and callus was maintained at pH 5.0, 6.5, 7.0 under control light conditions. The callus extract was harvested to reduce the silver ion and form AgNPs. It was observed that under controlled light conditions and at standard pH 5.7, best callus was formed with optimum pigmentations and synthesized AgNPs from this callus demonstrated highest antimicrobial activity against six different microbes. Furthermore, these AgNPs were characterized by using different analysis methods viz. UV-Visible analysis, XRD, EDX, SEM, TEM, AFM, DLS and FTIR to determine size, morphology, dispersity and functional groups. This research work seeks to pioneer in producing nanoparticles through a greener, rapid and cost-efficient method that can control the attributes of nanoparticles so they can be developed as a potent weapon against multi-drug resistant microbes.

Keywords: Physiological conditions; Callus; characterization; monodispersity; antimicrobial efficacy.

Received 12.10.2020

Revised 28.12.2020

Accepted 04.02. 2021

Introduction

In modern times, silver nanoparticles are being extensively used in food industry, biomedics, agriculture improvement, cosmetics, nanoelectronics and so on (1). The chemical and physical methods to produce nanoparticles prove to be expensive and hazardous to environment. Thus there is urgent need to choose biological route which is non-toxic, reliable, high yielding, rapid and feasible and also to identify plants rich in bioactive compounds. In the present study, AgNPs were developed from *in-vitro* grown *C. roseus* through callus extract route under controlled conditions. The metabolites (Terpenoids-indole alkaloids (TIA) : Vincristine, Vinblastine, Ajmalicine, Catharanthine and Serpentine) present in *C. roseus* extract act as reducing and stabilizing agents. Different physiological parameters (light and pH) were also applied to regulate the morphology of nanoparticles. The AgNPs with controlled structures that are uniform in size and shape and morphology, are successfully used in many biomedical applications (2, 3). The study also focuses on polydispersity of synthesized nanoparticles which had always been a challenge.

To determine and confirm the size, morphology, dispersity, purity, composition of different phases, presence of various functional groups and metal composition of the synthesized nanoparticles, several characterization techniques were used viz. UV-Vis spectroscopy, XRD, FTIR, DLS, SEM, TEM and AFM (4, 5, 6).

Previous studies suggested that smaller sized particles are more toxic as compared to bigger particles due to their large surface area. Nanoparticles may overcome limitations of existing antibiotics by combating multi-drug resistant bacteria. These tiny AgNPs are capable of entering in microbial cells and rupturing the cell wall, which leads to cell death. AgNPs have been used against pathogenic and multidrug-resistant bacteria, anti fungal agent and also as an anticarcinogenic agent against different cancerous cells. These AgNPs produce free radicals in bacterial cell and arrest the cell division of bacteria

by binding with biomolecules responsible for cell development. This study further test the biosynthesized silver nanoparticles to be explored as a potent antibacterial agent against different bacterial strains.

MATERIAL AND METHODS

Sample Preparation

For establishment of callus culture, leaf explants were collected from *in vitro* developed plantlets of *C. roseus* and cultured on MS media. For the ongoing research, cultivars of *Catharanthus roseus* seeds were obtained from the local nursery located in Gwalior city, country: India. Then the seeds were surface sterilized and treated with 0.1 % mercuric chloride for 1-2 min and kept under in-vitro conditions for 4 -5 weeks and inoculated on MS medium according to the method (7).

Preparation of Media for callus induction

For in-vitro cultivation of seed, MS medium was prepared and its pH was adjusted to 5.7. Then the solution was autoclaved at 121°C temp. and 15 pounds/inch pressure for approx. 20 min. and filter sterilized PGR were added into it.

Surface sterilization of Leaf Explants

The leaf explants were surface sterilized by treating with 1% Tween 20 and then washed with with 70% ethanol for around 5-10 minutes (7). Finally explants were surface sterilized with 0.1% mercuric chloride for around 8 minutes and then using autoclaved water (8).

Callus Formation

These explants were cut into tiny parts (mm) and then transferred into the MS media having varied levels of cytokinins and auxins (NAA 1mg/ml + BAP 3mg/ml). After the solution is kept for three weeks, incubation occurs which is marked by friable greenish and nodular callus (9).

The effect of various physiological conditions such as photoperiods and pH on growth and development of callus were observed and the best obtained callus was collected for the biosynthesis of NPs.

Biosynthesis of Ag NPs from callus extract

Firstly, the Callus was dried and finely powdered and then dissolved in 100 ml of sterilized water and kept overnight (10). Then the filtered extract was centrifuged at 3000 rpm for 20 min at 25°C. After the centrifuge is completed, the transparent part which floats above is collected for the synthesis of AgNPs.

During synthesis of AgNPs, a beaker containing 90 ml of AgNO₃ (1mM) was taken and 10 ml of the extract was added to it. The above formed mixture was then heated at 80 °C for around 30 minutes. After 30 minutes, the appearance of the solution changed from yellowish colour to a dark reddish brown colour, which indicated the formation of AgNPs. Now these freshly prepared nanoparticles were kept overnight in a cool dark place (11).

Characterization Process of AgNPs

There are multiple physicochemical techniques that are used to determine various physicochemical attributes of nanoparticles (12).

UV-Vis spectra analysis: A double beam UV-Visible spectrophotometer Shimadzu UV- 2450 Japan, was used to determine absorbance intensity of silver nanoparticles in the SPR band. The results obtained were in the range of 300 - 600 nm.

XRD analysis: X-ray diffractometer, Rigaku-miniFlex600 was operated at 40 kV and 30 mA and at 2 θ angle pattern with scanning range of 20^o - 80^o. average particle size is determined by the Debye-Scherrer equation $D = 0.9 \lambda / \beta \cos\theta$

FTIR studies: Perkin- Elmer FTIR-105627 USA was used to find out the presence of functional groups and secondary metabolites that are present on the surface of nanoparticles. The purified nanoparticles were mixed with 10 mg of potassium bromide powder and then the mixture was dried to remove the moisture content and a dried powder sample was prepared for analysis.

DLS analysis: Nano plus – Zetasizer was used to determine polydispersity index (size distribution profile) of the biosynthesized nanoparticles. 500 μ l of nanoparticles solution was taken and then diluted with 3 ml of sterilized distilled water. This solution mixture was then poured into the zeta dip cell and intensity was recorded vs time by the instrument which gave the size distribution of NPs.

AFM analysis: Instrument named NT-MDT, Russia was used to determine the surface topology and 3-D image of synthesized silver nanoparticles. It uses sharp probe for surface imaging at a very high resolution.

For the analysis, few drops of silver nanoparticles solution was placed on the glass slide and dried for around 15 minutes. This develops a thin film of the colloidal solution over the glass slide which is analyzed by AFM.

TEM and EDX analysis: Model-LV6490, manufacturer JEOL, was used to determine the size, morphology and elemental composition of nanoparticles. In this analysis, few drops of AgNPs solution was placed on

the grid (made of copper with carbon coating over it) and dried under a mercury lamp. A thin film of the colloidal solution forms and analyzed under EDX and TEM.

Determining Antimicrobial activity of AgNPs

MIC method

Inoculums sized fresh colonies of bacteria having concentrations of 10^{-5} , 10^{-6} , 10^{-7} CFU/ml were taken and inoculated on MHB. Serially diluted bacterial concentrations were made by mixing 9ml MHB and 1 ml of 10^{-5} , 10^{-6} , 10^{-7} bacterial concentrations serially and then incubated for 24h at 37 °C with 200 µg/ml concentration of AgNPs by the MIC method. The antimicrobial activity of biosynthesized AgNPs on Gram (+)ve and Gram (-)ve bacteria was determined against 200 µg/ml concentration of silver nanoparticles. The growth curve of bacterial cells in liquid medium containing AgNPs is examined and measured by taking OD at 590 nm.

Disc Diffusion Method

The antibacterial activity of AgNPs was determined against six different pathogenic bacteria (*Staphylococcus aureus* 9760 MTCC, *Streptococcus pyogenes* 1926 MTCC, *Bacillus cereus* 430, *Pseudomonas aeruginosa* MTCC 424, *Proteus mirabilis* MTCC 3310 and *Escherichia coli* MTCC 40) by the standard disk diffusion method. Whatman filter paper no.1 disks containing 100, 150 and 200 µg/ml of AgNPs combined with 10µg/ml streptomycin per disk were used for the test. MHA was used for bacterial growth. The overnight grown bacterial cultures were serially diluted to (1×10^{-7} CFU). After 24 hrs of incubation at 37 °C; synergistic antibacterial assay of the AgNPs and streptomycin were measured in terms of the diameter of ZOI around the filter paper disks.

RESULT AND DISCUSSION

Callus induction from leaf explants

Effect of different concentration and combination of growth hormones on callus induction

Callus induction is very important part in plant tissue culture and it depends on growth hormones, explants size and culture conditions. In this study, leaf explants were selected for callus induction. Different concentration of growth hormones was added in MS medium. Without any growth hormone, MS medium was unable to induce callus. BAP and NAA showed stimulatory effects on the callus induction (Table 1; Fig. 1). The highest percentage of callusing response in leaf (90%) was observed at 3:1 mg/l for BAP and NAA, respectively. Whereas, at a concentration of 4:3 mg/l (BAP and NAA respectively), 50% callus was observed in explants. Hence, combination of 3:1 mg/l (BAP & NAA) was suitable for the optimum induction of the callus in MS medium. Similar results were also reported in *Curcuma domestica* rhizomes (13).

Effect of different physico- chemical parameters (pH & photoperiod) on callus growth

To observe the effect of alteration in pH, callus was incubated on MS media with 3:1 BAP & NAA with different pH (5.0, 5.7, 6.5, 7.0) (Fig. 2) under control light conditions.

In another experiment, to observe the effect of alteration in photoperiods, callus was grown in same media composition and pH 5.7 but varying photoperiod conditions such as under controlled (16 hrs light and 8 hrs dark), SD (16 hrs dark and 8hrs light) and LD (20hrs light and 4 hrs dark).

The calluses were harvested at 7 and 14 days for further investigations (Table 2).

Effect of pH on media for callus development

Plant cells need suitable pH for better growth and development under in-vitro conditions. The pH of media can change the nutrient, hormonal and enzymatic activities as well as solidification of media. The pH level of media adjusts the cell metabolism and induces the cell division in shoot and root. At different pH condition, the growth of callus was inhibited at pH 5.0; pH 6.5 and pH 7.0 which indicates that high and low pH inhibit the growth of callus. However, the more inhibitory effect was observed at high pH. The fresh weight of the callus was recorded twice at pH 5.7 and less at pH 6.5 and pH 7.0 (Fig. 2). Not many differences were observed at pH 5.0.

Pigmentation is also a major morphological character which regulates the colour of callus. Change in pH of media significantly influenced the pigmentation of callus (Fig. 2). After 18-20 days of inoculation of callus on different media, callus was friable and white to light green at pH 5.7, while the yellow pigmented callus was observed at pH 5.0 after 25 days. At pH 6.5, callus was appearing cream to dark brown after 30 days and at pH 7.0 faded darks brown of the callus formation after appeared after 40 days of inoculation. Furthermore, it was observed that pH lower or higher than 5.7 also affected the formation of callus from explants cultures. Development of callus from leaf explants takes around 14 days at pH 5.7, 25 days at pH 5, 30 days at pH 6.5 and 40 days at pH 7.0. Based on these results, it was concluded that the pH of media is also responsible for delay in callus formation.

The pH also affects the condition of the solidifying agent in a medium. When the pH > 6, it produces a hardened medium and if pH < 5, it does not sufficiently solidify the medium.

Effects of different photoperiods on callus development

Light plays a crucial role for growth and development of callus. Table 2 illustrates the effect of various light conditions on callus culture growth. Control light conditions were observed to stimulate the photosynthetic mechanism within the cells of the induced callus and pigments began to produce which helped them gain autotrophy. Under both light and dark conditions, all essential substances for plant growth such as proteins, carbohydrates and various primary and secondary metabolites are being produced by these cells of induced callus. As far as the callus morphology is concerned, callus grown under light conditions were found to be much more compact than that of callus grown under dark conditions (Table 2)

The study observes the growth of Callus when exposed to different amount of light for varied time intervals, viz. under the control condition and followed by SD and LD and duration ranging from 7 to 14 days. When exposed to various lighting conditions, significant changes could be observed during the development of greenish callus. At pH 5.7 in the medium, and comparing all the growth conditions under observation, it was found that at control condition, the growth was rapid and the callus formed was compact and looked greenish. During SD and LD, the growth of callus was hampered which indicates that less and excess exposure to the amount of incident light can inhibit the callus growth. The fresh weight of callus was double in case of controlled light conditions as compared to fresh weight of callus incubated at LD and was also greater in amount than that of callus grown in SD. The above conclusion suggests that reduction in the amount of light does not provide favorable atmosphere for the growth and development of callus.

Altering the light conditions from controlled to SD as well as LD, drastic differences were noticed in the colour of the pigment generated in the callus (Table 2). After 7 days of treatment, under control conditions which provided favorable conditions for growth, callus turned greenish in colour which indicated greater survival. 14 days of treatment of same callus gave similar kind of results. When callus was put in observation for 7 days under SD, colour of callus turned to brown and yellow owing to the accumulation of phenols. When the treatment was increased to 14 days, callus got in decline phase because of the gradual decrease in photosynthesis reaction. When put under LD for 7 days, callus appeared brown, and after 14 days, its colour changed into brownish to black type (Table 2). The above results suggested that the control condition generated a healthy callus whereas when callus was put under SD and LD condition, the phenols started to accumulate and they gave a brown and black pigment to the callus. The results that we obtained above agree with the work published (14). Their work included the study of induction and growth of callus in various light and dark conditions.

Optimum callus formation from leaf (91%) was observed when the leaf cultures were maintained under 16/8 hrs (light and dark) (Table 2). Exposure to short days had reduced the percentage of callus formation from leaf from 91% to 79 % whereas on exposure to long days further decreased to 60 %.

A histogram bar graph was generated to analyze the correlation between different light conditions and callus growth rate when treated with 7 and 14 days (Fig. 3. A, B, C).

Growth index

Callus tissues were harvested at the age of 7, 14 days and different pH 5.0, 5.7, 6.5 and 7.0 and their growth indexes were calculated on fresh weight basis (Fig. 3.A,B,C) using following formula: $GI = \frac{\text{Final weight of tissue} - \text{Initial weight of tissue}}{\text{Initial weight of tissue}}$

To make fresh weight determination, Callus culture was slowly pressed on the Whatman filter paper no.1 to remove extra water. All experiments were replicated three times.

Characterization of AgNPs from callus formed under different photoperiods and pH

UV Spectroscopy Analysis

The UV-Visible spectroscopy is one of the most effective tools to evaluate the size and shape of the AgNPs (15). Ag NPs were synthesized by using CME incubated at different photoperiods at pH 5.7. At 7 days of incubation, control-CME was mixed with silver nitrate solution, a colour change from transparent yellowish to light yellow and finally a colloidal light brown was observed (Fig. 4 A). When 14 days control-CME was mixed with silver nitrate, dark yellow extract changed into dark brown colour suspension, which proves the formation of AgNPs (Fig. 4 B). Then this formation of AgNPs was examined by measuring the absorption spectra at regular time intervals. For NPs from 14 days control-CME, the peak was observed at 420 nm and widening of the peak indicated that the particles were monodispersed. On the contrary, in SD and LD cases of 7 & 14 days incubation absorbance peak was found outside the SPR band (Fig. 4: A&B). When the nanoparticles synthesis increases, the SPR intensity also increases (16, 17). Ahmad et al. reported that light is one of the major elicitors which fluctuate morphogenic potential, biochemical reactions and secondary metabolite production (18).

pH is an important media factor which affect the callus formation, morphology etc due to alternation of metabolites of callus. Ag NPs were synthesized by using callus mediated extract at different pH 5.0, 6.5, 7.0. The formation of nanoparticles was confirmed by the changes in colour of CME suspension into grayish colour, brownish colour and dark grayish colour at different pH. (Fig. 4 C) shows UV-Visible spectra analysis in which peaks were observed at 459nm, 454nm and at 452nm at pH 5.0, pH 6.5 and pH 7.0. These peaks were not found within the SPR band and hence were polydispersed nanoparticles which were inefficient as antimicrobial agents.

XRD

The crystalline nature of AgNPs was determined by X-ray diffraction study. At pH 5.7 and at 7 days, AgNPs synthesized from control-CME, showed the XRD at 27.9° , 32.38° , 38.32° , 46.34° , 54.0° , 64.76° and 67.72° which can be indexed to (110), (111), (200), (211), (220), (311) and (222) respectively (Fig. 5 A). Whereas, at 14 day XRD spectra of AgNPs owed peak at 27.78° , 32.18° , 38.24° , 46.18° , 54.82° , 64.52° and 67.34° corresponding to (110), (111), (200), (211), (220), (311) and (222) respectively (Fig. 5 B). Peaks and its corresponding angles for SD- CME (7& 14days) and LD-CME were recorded and average particle size was calculated using the Debye Sherrer's formula (19, 20). These all peaks were corroborated with the standard silver nanoparticles (JCPDS file no. 12-0793). Similarly, all the results of highest intense peaks were found at (111) and (110). The Average particle size of Control-CME of AgNPs (at 7 & 14 days) was 32.38 nm and 16.09 nm whereas average size of 35.65 nm and 16.14 nm were obtained from 7 & 14 days (SD) of AgNPs. In case of 7 & 14 days (LD) of AgNPs average sizes were 36.11 nm and 16.19 nm, respectively. The smallest sized nanoparticles were found to be in Control-CME based AgNPs.

Fig.5: C represents the XRD pattern of the AgNPs synthesized by callus mediated extract at pH 5.0, 6.5 and 7.0. The diffraction peaks data found were in accordance with the reports of FCC structure from JCPDS file No. 04-0783. Impurities could be observed (marked by * against the peak) in all the pH (5.0, 6.5, 7.0) in the formation of nanoparticles (Fig.5: C) and intensity against the peak is also low which indicated that nanoparticles formed by CME at these pH does not exhibit crystalline nature. Hence the best pH was found to be 5.7 with callus extract under controlled light conditions.

FTIR

Fig. 6 A shows, the FTIR spectra of control-CME silver nanoparticles indicated peaks at 7 days, around 3440 , 2924 , 1731 , 1637 , 1384 , 1032 , 698 and 667 cm^{-1} which correspond to the groups O-H stretch, C-H stretch, C=O Stretch, -C=C-stretch, -C-H variable, C-F Stretch and C-Cl whereas at 14 days AgNPs of control-CME showed the peaks which were close to 7 days results. The peaks obtained from SD-CME and LD-CME at 7 & 14 days gave peaks which represented the same aforementioned functional groups (Fig. 6: A&B).

It is thus evident from FTIR spectra of the AgNPs that the bioactive compound such are polyphenols, flavanoids, flavones, which are earlier reported in *Z.mays* plays a very significant function in the stabilization and capping of the AgNPs by reducing Ag metal ion (21, 22, 23). The methyl group and asymmetric starching band were present in control-CME Ag NPs (24). This is may be due to the strong binding of amino acids to the AgNPs surfaces and robust capping by the proteins and polysaccharides in the extract of control-CME.

The FTIR measurements of synthesized silver nanoparticles by using CME for pH 5.0, pH 6.5 and pH 7.0 did not give proper peaks (Fig. 6 C) because secondary structure of proteins was not affected during the reaction of silver ion into AgNPs.

EDX

EDX analysis of AgNPs shows the elemental composition of Ag and chlorine (Cl) and confirms the presence of metallic Ag in the biosynthesized AgNPs. 17.66 % chlorine and 82.34% silver were reported in control-CME at 7 days at pH 5.7 (See Fig. 7: A1), whereas 18.09 % chlorine and 81.91% silver were reported in control-CME at 14 days (See Fig. 7: B1). In case of SD and LD (both 7&14 days) the composition of silver dropped due to different light treatment on the growth phase of callus (Fig. 7: A2, B2, A3, B3).

During this phase, bio-organic molecules, such as polysaccharides, phenols, and proteins of callus extract which act as reducing, stabilizing and capping agents broke down.

Fig. 7: C1-C3 shows EDX image of the biosynthesized AgNPs at different pH 5.0, 6.5, 7.0. Lower compositions of silver and higher amount of other undesired elements (impurities) such as C, O, Si, S were found. Lower the silver least effective would be the formed silver nanoparticles.

DLS

Fig. 8 shows the particle size of the AgNPs using control-CME at 7 & 14 days at pH 5.7 which was found to be 14.11 nm and 15.12 nm respectively (See Fig. 8: A1 & B1). It was clearly indicated that the obtained AgNPs are monodispersed in nature. In the case of SD-CME and LD-CME, the size of AgNPs was obtained

103 nm and 100 nm respectively (See Fig. 8: A2 & A3). This indicated huge difference in size range of nanoparticles. Smaller nanoparticles demonstrated greater antimicrobial efficacy.

Fig. 8: C1-C3 shows the DLS data for the AgNPs prepared from CME at different pH 5.0, 6.5, 7.0 under standard light conditions (16 hr light & 8 hrs dark). Large sized nanoparticles were formed at these pH viz 362nm, 318nm, 817nm respectively in comparison to tiny nanoparticles formed at pH 5.7 (14.11nm).

AFM

The AFM 3D images indicate the uniform distribution and topology of synthesized AgNPs. During this analysis, AgNPs from CME under Control, Short days and Long days was compared only for 7 days and at pH 5.7 (See Fig. 9: A,B, C). Size of nanoparticles were found to be approximately same for 14 days when observed under other characterization techniques, hence analysis for 14 days was not considered in this technique. AFM shows the Granularity accumulation distribution (GAD), which gives the particle size distribution of AgNPs. AFM analysis exhibited the size of the NPs 20-40 nm for control-CME Ag NPs (Fig. 9: A). Results prove that AgNPs were monodispersed and homogeneously distributed. For SD-CME and LD-CME, size of silver nanoparticles ranged from 100-120 nm and 150-170 nm respectively (Fig. 9: B&C). The large diameter as in SD and LD could be due to sedimentation of the particles resulting in a decrease in absorbance (Delay et al. 2011). Images revealed smooth surface, needle shape and compact structures. For SD and LD particles were observed with less concentration of silver nanoparticles and show heterogeneous size and polydispersity.

Fig. 9 (D, E & F) shows analysis of synthesized AgNPs using callus mediate extract at pH 5.0, pH 6.5 and pH 7.0. Nanoparticles have an average diameter of 120 nm, 140 nm and 150 nm for pH 5.0, 6.5 and 7.0 respectively. These large sized nanoparticles were found to be inefficient for antimicrobial activity.

TEM analysis

The silver nanoparticles synthesized by control-CME at 7 days formed at pH 5.7 were observed using TEM and the particle size were found at average size of 19.13 nm (Fig. 10: A1-A4) and spherical. For the synthesized AgNPs using SD 7 days, particles are spherical, but not uniformly distributed and were agglomerated and also showed sticky nature (Fig. 10: B1-B4). Average size of particles was 68.09 nm. For the synthesized AgNPs using LD 7 days, the average size of AgNPs was measured to be 28.49 nm but the particles were mostly elliptical in shape and polydispersed in size distribution and observed dense form (Fig. 10: C1-C4). The size histograms showed a Gaussian distribution.

The SAED patterns of AgNPs further demonstrate the crystalline nature of NPs which have already been defined by XRD. The intermittent bright dots arranged in concentric Debye-Sherrer rings can be indexed to the peaks of XRD as (110), (111), (200), (211), (220), (311) and (222) for all of the synthesized AgNPs using 7 days Control, SD and LD. The particles size observed under TEM study is close to that of the XRD study.

The green synthesized AgNPs using 7 days (control condition) callus extract had a size range from 5 to 30 nm by applying the histogram data with a Gaussian distribution centered at 19.13 nm with 0.53 nm of standard deviation (Fig. 10: A4). It has been observed that NPs of small sizes have been recorded in monodispersed form (Fig. 10: A3). The results of the average particle size and distribution procured from TEM analysis matches well with DLS analysis. For crystalline degree of NPs, HRTEM and SAED were done. During the growth phase, small adjacent NPs easily aggregate into large size particles which increase the thermodynamic stability of NPs. These determine the final shape of the NPs in the process termination phase (25, 26). However, as the growth phase increases, there are nanoprisms, nanotube, nano hexahedrons, and other irregularly shaped NPs formed by aggregation (27, 14). In the end phase, NPs obtain the most energetically favorable structure, which strongly influences the ability to stabilize metal NPs during the whole process.

The presence, absence, timing and intensity of light play a significant role in explants morphogenesis (28) and directly affects the catalytic and anabolic processes, especially secondary metabolism (29, 30). Light also influences callogenesis (31). Changing period of 16hrs light and 8hrs dark exposure to white light is superior to a continuous light exposure (7). Moreover, dark exposure can be related to negative effect in some species *Nicotiana tabacum* anthers produced less callus and fewer embryoids (32, 28).

Antimicrobial activity of silver nanoparticles and synergistic activity

Disk diffusion method by ZOI

The result shows that AgNPs undergo a contact with the bacteria cell and shows a strong and effective antibacterial activity against Gram (+) ve bacteria compared to Gram (-) ve bacteria. The formation of a clean area around the disk exhibits antibacterial activity (Fig. 11) which is termed as ZOI. Control-CME AgNPs (7 & 14 days and at pH 5.7) at a concentration of 200µg/ml when used individually showed moderate antibacterial activity against six pathogenic bacteria and produced ZOI of 12.98 diameter and 13.00 mm diameter respectively (Table 3 & Fig. 11 A).

In this study, SD-CME AgNPs (7 & 14 days) showed a very less ZOI against three of the six bacteria and no inhibitory effect was observed against remaining three (Table 4 A). LD-CME AgNPs (7 & 14 days) did not show inhibition zone against any of the six bacteria (Table 4B).

AgNPs synthesized from CME at pH 5.0, 6.5 and 7.0 with controlled light conditions were unable to demonstrate antimicrobial activity against any of the microorganisms at any concentrations (Table 5).

The standard antibiotic, streptomycin at concentration 10µg/ml did not show very good activity against the tested pathogens. However, the combined effect of antibiotics and AgNPs from control CME 7 & 14 days, displayed strong antibacterial activity against all the tested pathogens at 200 µg/ml, with a ZOI ranging in diameter from 16.03 to 17.37 mm for 7 days and 16.12 to 17.98 mm for 14 days (Table 3 & Fig. 11 A). Additionally, at 200µg/ml concentration, the zone of inhibition obtained against gram-positive bacteria (*B. cereus* 430 MTCC) was more as compared to gram-negative bacteria (*E. coli* 40 MTCC).

In Case of LD-CME AgNPs (7 & 14 days) with antibiotics, they did not show any antibacterial activity against each bacteria at 200µg/ml, 100µg/ml and 150µg/ml (Table 4B & Fig. 11 C) . Similar results were obtained for SD-CME AgNPs (7 & 14 days) (Table 4A & Fig. 11 B).

Antimicrobial activity by MIC Method

Fig. 12 shows the MIC values of 200µg/ml AgNPs as calculated by optical density at 590 nm wavelength. Higher concentration of AgNPs (Fig. 12 A-C) was found to inhibit bacterial growth completely than lower concentrations. Finally, for AgNPs of *C.roseus*, the average MIC value was 200µg/ml for both Gram (+)ve bacteria and Gram (-)ve bacteria. However, in the present study of 7 & 14 Days treated callus (controlled light and at pH 5.7), bactericidal activity of AgNPs was higher in Gram (+) ve bacteria compared to Gram (-) ve bacteria. (Fig. 12 A).

This is due to the fact that the cell wall of the Gram-positive bacteria binds the metals in large quantities as compared to the Gram-negative bacteria (33). Small-sized AgNPs are more bactericidal than the larger ones. In case of AgNPs from SD-CME and LD-CME, there was no inhibition of bacterial growth against any of the six pathogens.

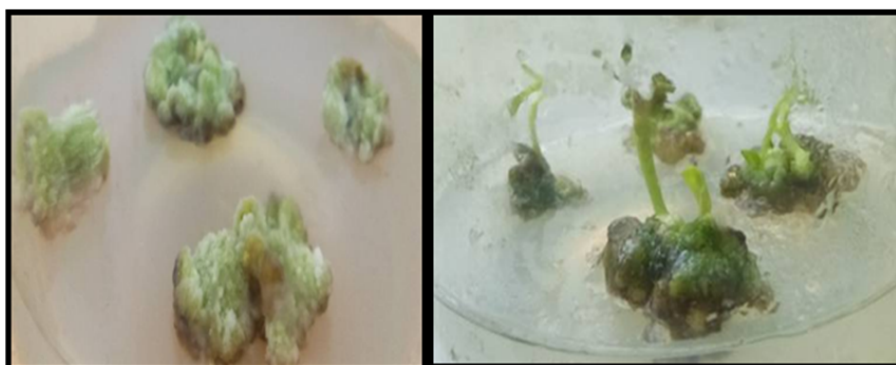


Figure 1: Callus induction from leaf explants with the help of NAA and BAP.



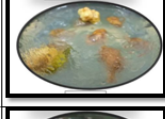

Figure	pH of media	Explants	Observation
	5.0	Leaf	Yellow callus formation after 25 days
	5.7	Leaf	White to light green callus formation after 14 days
	6.5	Leaf	Cream to dark brown callus formation after 30 days
	7.0	Leaf	Faded dark brown of the callus formation after 40 days

Figure 2: Growth of callus under different pH.

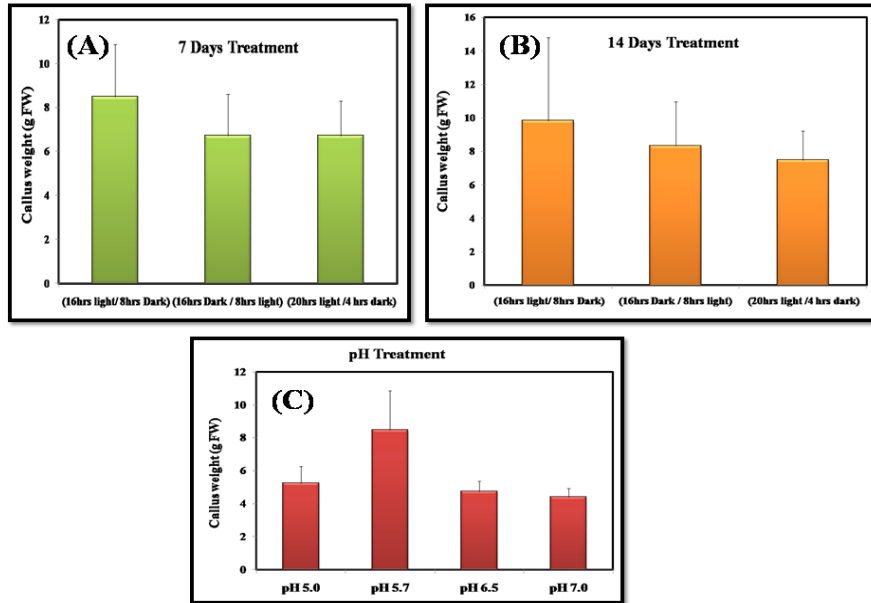


Figure 3: Callus weight changes under different light and pH conditions. During the (A) 7 Days (B) 14 Days (C) Different Ph. Results are expressed as Mean± S.E.

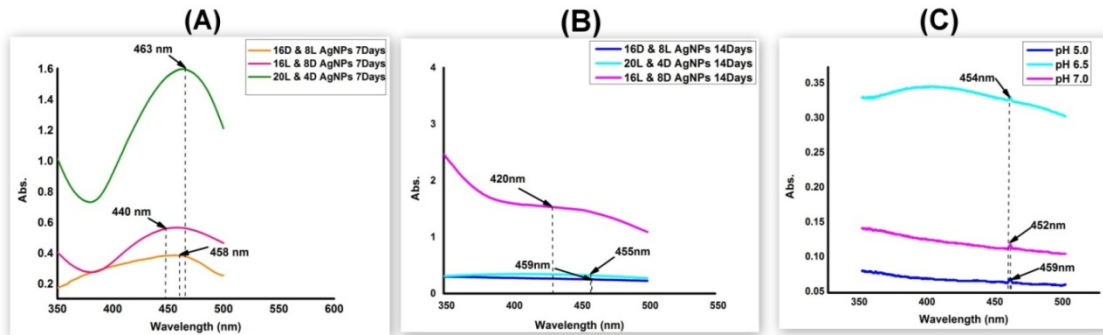


Figure 4: UV-visible spectra (A) 7 Days (B) 14 Days (C) Different pH.

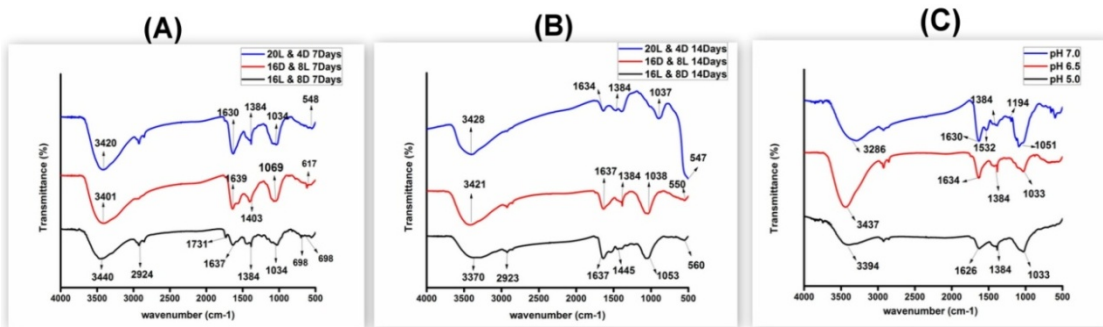


Figure 5: XRD (A) 7 Days (B) 14 Days (C) Different pH.

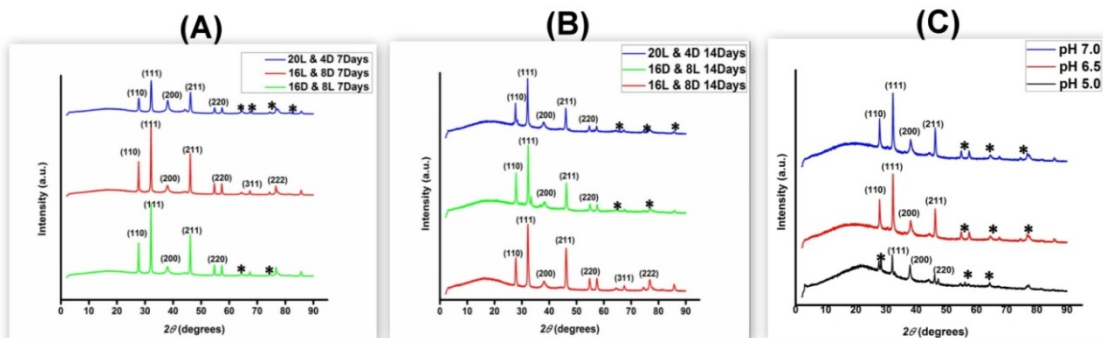


Figure 6: FTIR (A) 7 Days (B) 14 Days (C) Different pH.

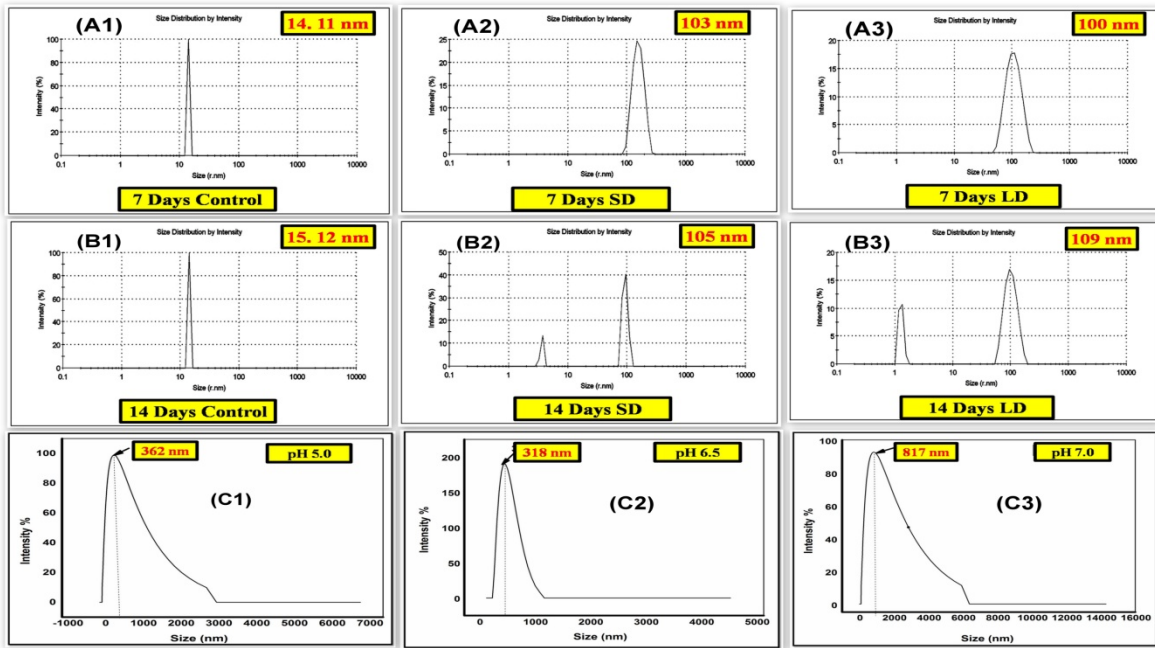


Figure 7: EDX analysis (A1-A3) 7 Days (B1-B3) 14 Days (C1-C3) Different pH.

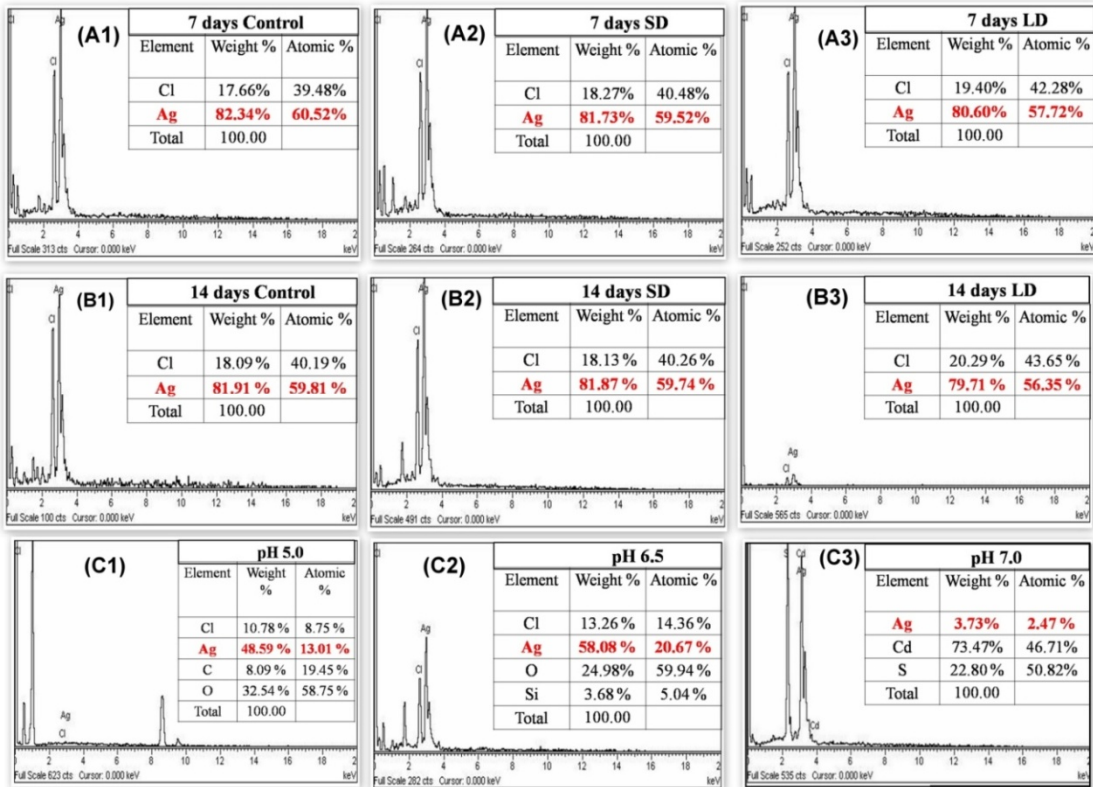


Figure 8: Particle size distribution (A1-A3) 7 Days (B1-B3) 14 Days (C1-C3) Different pH.

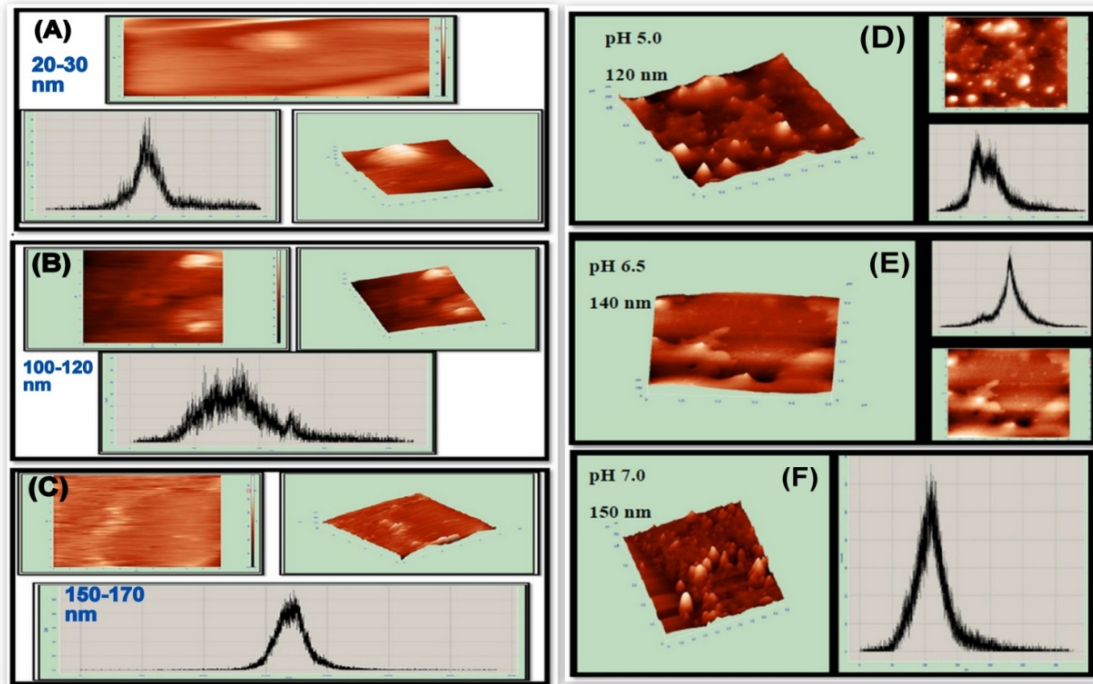


Figure 9: AFM images (A) Control (B) SD (C) LD (D-F) Different pH.

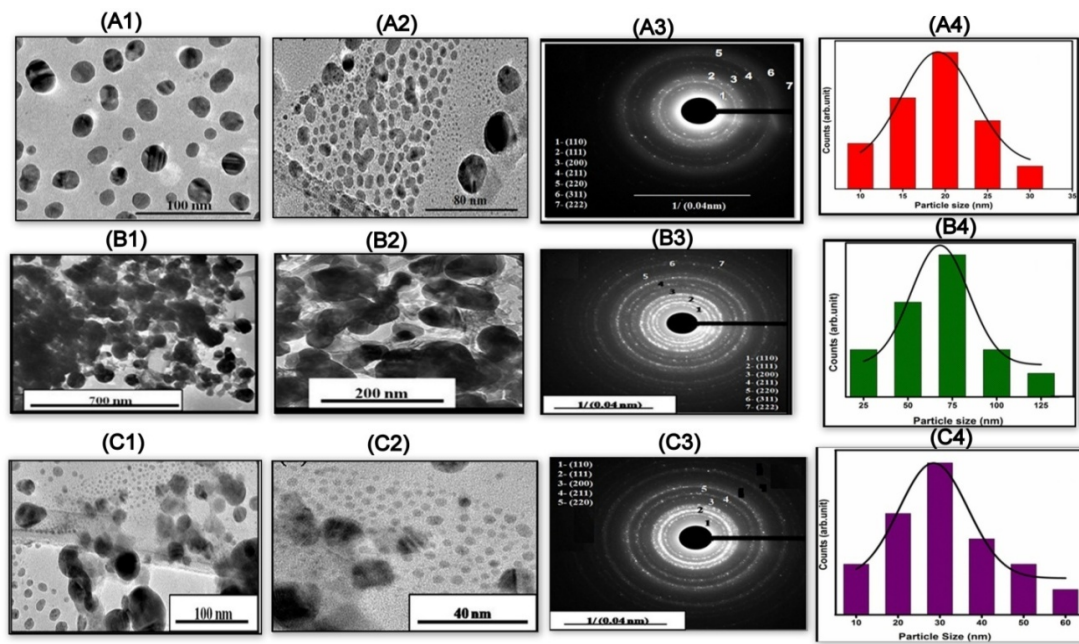


Figure 10: (A1-A4) 7 Days (B1-B4) 14 Days (C1-C4) Different pH.

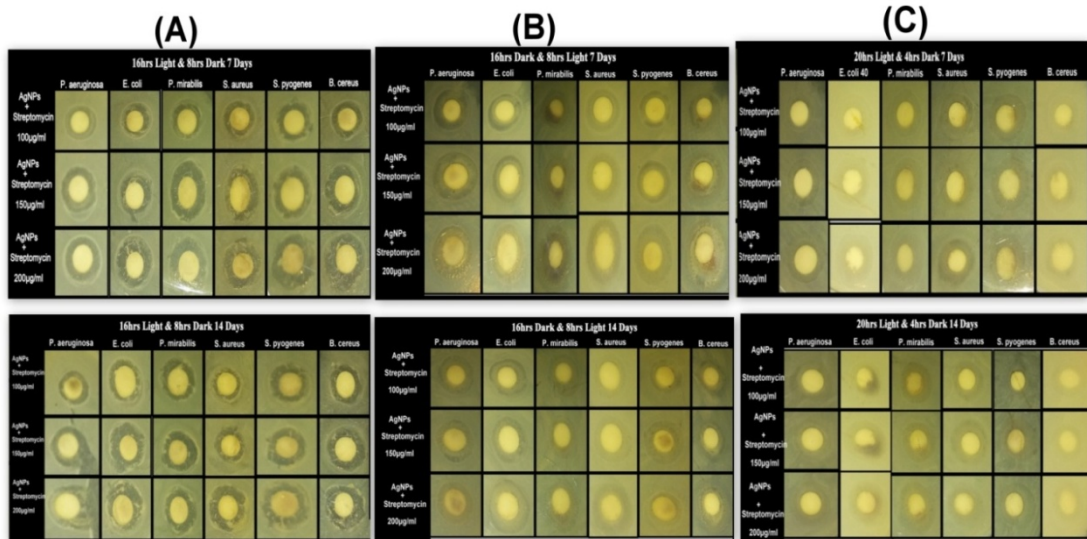


Figure 11: Antibacterial activity of 7 & 14 Days treated (A) Control, (B) SD (C) LD AgNPs (100,150 and 200µg/ml) and compared to AgNPs combined with antibiotic- streptomycin (10µg/ml) by ZOI measurement.

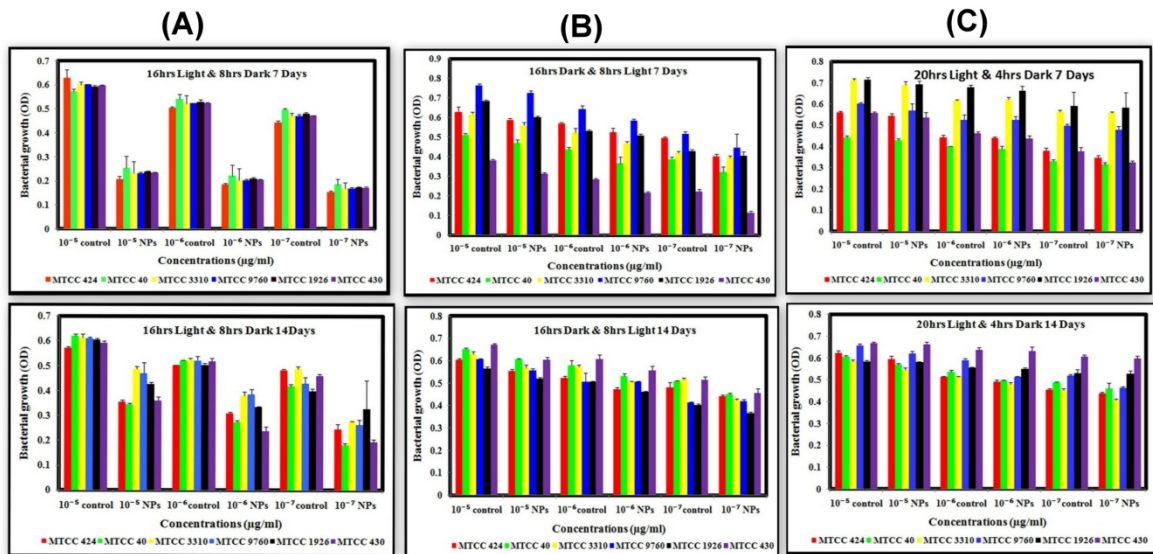


Figure 12: 7 & 14 Days treated (A) Control, (B) SD (C) LD AgNPs 200µg/ml against microbes (Gram positive & Gram negative). Results are expressed as Mean± S.E.

Table 1.: Standardization of callus induction from leaf explants using different concentration of BAP and NAA mg/l

Concentration of growth hormones		Leaf	
BAP	NAA	% of callus induction	Initiation of callus (Days)
0.5	0.5	20%	25
1	1	60%	18
1.5	2	70%	15
3	1	90%	13

Table 2.: The effects of light exposure on leaf explants, cultured on MS media (1.0 mgL⁻¹ NAA + 3.0 mgL⁻¹ BAP) at 25 ± 1°C.

Light exposure (hrs)		Explants	Observations	Callus (%)
Light	dark			
16	8	Leaf	Green callus formation	91%
8	16	Leaf	Yellow callus formation	79%
20	4	Leaf	Black callus formation	60%

Table 3: Antibacterial activity of synthesized AgNPs and synergistic activity streptomycin against pathogenic bacteria (Data shown in zone of inhibition in mm.

16hrs Light & 8hrs Dark 7 Days					
Bacteria	Streptomycin (10µg/ml)	Single Concentration of AgNPs 200µg/ml	AgNPs 100µg/ml + Streptomycin	AgNPs 150µg/ml + Streptomycin	AgNPs 200µg/ml + Streptomycin
<i>P. aeruginosa</i> MTCC 424	11.03 ± 0.03	12.09 ± 0.01	13.98 ± 0.04	14.08 ± 0.11	15.03 ± 0.83
<i>E. coli</i> MTCC 40	10.07 ± 0.94	12.98 ± 1.19	14.60 ± 0.01	15.08 ± 0.03	16.03 ± 0.03
<i>P. mirabilis</i> MTCC 3310	10.88 ± 0.10	10.59 ± 0.55	10.72 ± 0.22	11.20 ± 0.12	12.62 ± 0.52
<i>S. aureus</i> MTCC 9760	11.07 ± 0.00	11.78 ± 0.00	12.14 ± 0.01	12.53 ± 0.19	15.63 ± 0.15
<i>S. pyogenes</i> MTCC 1926	11.09 ± 2.17	12.12 ± 0.17	12.23 ± 0.00	13.52 ± 0.03	16.61 ± 0.03
<i>B. cereus</i> MTCC 430	11.03 ± 0.04	12.88 ± 0.01	13.99 ± 0.06	15.50 ± 0.02	17.37 ± 0.48

16hrs Light & 8hrs Dark 14 Days					
Bacteria	Streptomycin (10µg/ml)	Single Concentration of AgNPs 200µg/ml	AgNPs 100µg/ml + Streptomycin	AgNPs 150µg/ml + Streptomycin	AgNPs 200µg/ml + Streptomycin
<i>P. aeruginosa</i> MTCC 424	11.03 ± 0.03	12.12 ± 0.01	14.09 ± 0.04	14.15 ± 0.11	15.30 ± 0.83
<i>E. coli</i> MTCC 40	10.07 ± 0.94	13.00 ± 1.19	14.80 ± 0.01	15.21 ± 0.03	16.12 ± 0.03
<i>P. mirabilis</i> MTCC 3310	10.88 ± 0.10	10.91 ± 0.55	11.01 ± 0.22	11.29 ± 0.12	12.98 ± 0.52
<i>S. aureus</i> MTCC 9760	11.07 ± 0.00	11.90 ± 0.00	12.80 ± 0.01	12.88 ± 0.19	15.98 ± 0.15
<i>S. pyogenes</i> MTCC 1926	11.09 ± 2.17	12.30 ± 0.17	12.35 ± 0.00	13.60 ± 0.03	16.68 ± 0.03
<i>B. cereus</i> MTCC 430	11.03 ± 0.04	12.98 ± 0.01	14.01 ± 0.06	15.98 ± 0.02	17.98 ± 0.48

Table 4(A): Antibacterial activity of synthesized AgNPs and synergistic activity streptomycin against pathogenic bacteria (Data shown in zone of inhibition in mm.

16hrs Dark & 8hrs Light 7 Days					
Bacteria	Streptomycin (10µg/ml)	Single Concentration of AgNPs 200µg/ml	AgNPs 100µg/ml + Streptomycin	AgNPs 150µg/ml + Streptomycin	AgNPs 200µg/ml + Streptomycin
<i>P. aeruginosa</i> MTCC 424	11.01 ± 0.00	10.00 ± 0.00	10.21 ± 0.11	11.08 ± 0.11	11.15 ± 0.06
<i>E. coli</i> MTCC 40	10.74 ± 0.54	8.26 ± 0.06	10.74 ± 0.54	11.10 ± 0.11	11.15 ± 0.03
<i>P. mirabilis</i> MTCC 3310	10.07 ± 0.01	0.17 ± 0.05	0.03 ± 0.00	0.39 ± 0.34	0.04 ± 0.06
<i>S. aureus</i> MTCC 9760	11.03 ± 0.04	0.38 ± 0.51	0.12 ± 0.00	0.60 ± 0.02	11.38 ± 0.34
<i>S. pyogenes</i> MTCC 1926	11.03 ± 0.04	10.79 ± 0.40	11.03 ± 0.04	11.25 ± 0.00	11.25 ± 0.24
<i>B. cereus</i> MTCC 430	11.04 ± 0.04	0.11 ± 0.00	0.14 ± 0.00	0.53 ± 0.04	0.37 ± 0.25

16hrs Dark & 8hrs Light 14 Days					
Bacteria	Streptomycin (10µg/ml)	Single Concentration of AgNPs 200µg/ml	AgNPs 100µg/ml + Streptomycin	AgNPs 150µg/ml + Streptomycin	AgNPs 200µg/ml + Streptomycin
<i>P. aeruginosa</i> MTCC 424	11.01 ± 0.00	10.03 ± 0.04	11.16 ± 0.08	11.16 ± 2.17	11.16 ± 0.02
<i>E. coli</i> MTCC 40	10.74 ± 0.54	8.26 ± 1.05	9.57 ± 0.16	9.93 ± 0.93	10.30 ± 1.50
<i>P. mirabilis</i> MTCC 3310	10.07 ± 0.01	0.20 ± 0.09	0.07 ± 0.01	0.04 ± 0.04	0.04 ± 0.06
<i>S. aureus</i> MTCC 9760	11.03 ± 0.04	0.12 ± 0.04	0.01 ± 0.01	0.10 ± 0.08	11.50 ± 0.41
<i>S. pyogenes</i> MTCC 1926	11.03 ± 0.04	10.80 ± 0.02	11.23 ± 0.00	11.23 ± 2.17	11.46 ± 0.01
<i>B. cereus</i> MTCC 430	11.04 ± 0.04	0.04 ± 0.05	0.09 ± 0.07	0.14 ± 0.06	0.25 ± 0.07

Table 4(B): Antibacterial activity of synthesized AgNPs and synergistic activity streptomycin against pathogenic bacteria (Data shown in zone of inhibition in mm).

20hrs Light & 4hrs Dark 7 Days					
Bacteria	Streptomycin (10µg/ml)	Single Concentration of AgNPs 200µg/ml	AgNPs 100µg/ml + Streptomycin	AgNPs 150µg/ml + Streptomycin	AgNPs 200µg/ml + Streptomycin
<i>P. aeruginosa</i> MTCC 424	11.33 ± 0.47	0.00 ± 0.04	0.11 ± 0.07	0.20 ± 0.17	0.07 ± 0.01
<i>E. coli</i> MTCC 40	10.07 ± 0.94	0.19 ± 0.15	0.23 ± 0.28	0.27 ± 0.28	0.62 ± 0.52
<i>P. mirabilis</i> MTCC 3310	11.33 ± 1.05	0.11 ± 0.10	0.03 ± 0.00	0.45 ± 0.40	0.04 ± 0.06
<i>S. aureus</i> MTCC 9760	12.03 ± 0.07	0.38 ± 0.51	0.12 ± 0.00	0.03 ± 0.03	0.29 ± 0.42
<i>S. pyogenes</i> MTCC 1926	12.36 ± 0.45	0.12 ± 0.17	0.23 ± 0.00	0.03 ± 0.02	0.61 ± 0.32
<i>B. cereus</i> MTCC 430	12.46 ± 0.50	0.11 ± 0.00	0.14 ± 0.00	0.53 ± 0.04	0.37 ± 0.25

20hrs Light & 4hrs Dark 14 Days					
Bacteria	Streptomycin (10µg/ml)	Single Concentration of AgNPs 200µg/ml	AgNPs 100µg/ml + Streptomycin	AgNPs 150µg/ml + Streptomycin	AgNPs 200µg/ml + Streptomycin
<i>P. aeruginosa</i> MTCC 424	11.33 ± 0.47	0.00 ± 0.00	0.11 ± 0.07	0.20 ± 0.17	0.07 ± 0.01
<i>E. coli</i> MTCC 40	10.07 ± 0.94	0.10 ± 0.16	0.23 ± 0.28	0.27 ± 0.28	0.62 ± 0.52
<i>P. mirabilis</i> MTCC 3310	11.33 ± 1.05	0.01 ± 0.00	0.03 ± 0.00	0.45 ± 0.40	0.04 ± 0.06
<i>S. aureus</i> MTCC 9760	12.03 ± 0.07	0.03 ± 0.04	0.12 ± 0.00	0.03 ± 0.03	0.29 ± 0.42
<i>S. pyogenes</i> MTCC 1926	12.36 ± 0.45	0.02 ± 0.01	0.23 ± 0.00	0.03 ± 0.02	0.61 ± 0.32
<i>B. cereus</i> MTCC 430	12.46 ± 0.50	0.01 ± 0.00	0.14 ± 0.00	0.53 ± 0.04	0.37 ± 0.25

Table 5.: Antibacterial activity of AgNPs and synergistic activity with streptomycin against pathogenic bacteria (Data are shown in the zone of inhibition in mm)

pH 5.0					
Bacteria	Streptomycin (10µg/ml)	Single Concentration of AgNPs 200µg/ml	AgNPs 100µg/ml + Streptomycin	AgNPs 150µg/ml + Streptomycin	AgNPs 200µg/ml + Streptomycin
<i>P. aeruginosa</i> MTCC 424	11.33 ± 0.47	0.00 ± 0.00	0.01 ± 0.02	0.20 ± 0.01	0.02 ± 0.02
<i>E. coli</i> MTCC 40	10.07 ± 0.94	0.03 ± 0.00	0.07 ± 0.01	0.03 ± 0.03	0.12 ± 0.15
<i>P. mirabilis</i> MTCC 3310	11.33 ± 1.05	0.01 ± 0.00	0.03 ± 0.00	0.02 ± 0.03	0.00 ± 0.00
<i>S. aureus</i> MTCC 9760	12.03 ± 0.07	0.04 ± 0.03	0.04 ± 0.05	0.03 ± 0.03	0.03 ± 0.04
<i>S. pyogenes</i> MTCC 1926	12.36 ± 0.45	0.02 ± 0.01	0.03 ± 0.00	0.03 ± 0.02	0.05 ± 0.02
<i>B. cereus</i> MTCC 430	12.46 ± 0.50	0.01 ± 0.00	0.04 ± 0.00	0.20 ± 0.25	0.10 ± 0.08

pH 6.5					
Bacteria	Streptomycin (10µg/ml)	Single Concentration of AgNPs 200µg/ml	AgNPs 100µg/ml + Streptomycin	AgNPs 150µg/ml + Streptomycin	AgNPs 200µg/ml + Streptomycin
<i>P. aeruginosa</i> MTCC 424	11.33 ± 0.47	0.00 ± 0.00	0.01 ± 0.02	0.20 ± 0.01	0.02 ± 0.02
<i>E. coli</i> MTCC 40	10.07 ± 0.94	0.03 ± 0.00	0.07 ± 0.01	0.03 ± 0.03	0.12 ± 0.15
<i>P. mirabilis</i> MTCC 3310	11.33 ± 1.05	0.01 ± 0.00	0.03 ± 0.00	0.02 ± 0.03	0.00 ± 0.00
<i>S. aureus</i> MTCC 9760	12.03 ± 0.07	0.04 ± 0.03	0.04 ± 0.05	0.03 ± 0.03	0.03 ± 0.04
<i>S. pyogenes</i> MTCC 1926	12.36 ± 0.45	0.02 ± 0.01	0.03 ± 0.00	0.03 ± 0.02	0.05 ± 0.02
<i>B. cereus</i> MTCC 430	12.46 ± 0.50	0.01 ± 0.00	0.04 ± 0.00	0.20 ± 0.25	0.10 ± 0.08

pH 7.0					
Bacteria	Streptomycin (10µg/ml)	Single Concentration of AgNPs 200µg/ml	AgNPs 100µg/ml + Streptomycin	AgNPs 150µg/ml + Streptomycin	AgNPs 200µg/ml + Streptomycin
<i>P. aeruginosa</i> MTCC 424	11.33 ± 0.47	0.00 ± 0.00	0.01 ± 0.02	0.20 ± 0.01	0.02 ± 0.02
<i>E. coli</i> MTCC 40	10.07 ± 0.94	0.03 ± 0.00	0.07 ± 0.01	0.03 ± 0.03	0.12 ± 0.15
<i>P. mirabilis</i> MTCC 3310	11.33 ± 1.05	0.01 ± 0.00	0.03 ± 0.00	0.02 ± 0.03	0.00 ± 0.00
<i>S. aureus</i> MTCC 9760	12.03 ± 0.07	0.04 ± 0.03	0.04 ± 0.05	0.03 ± 0.03	0.03 ± 0.04
<i>S. pyogenes</i> MTCC 1926	12.36 ± 0.45	0.02 ± 0.01	0.03 ± 0.00	0.03 ± 0.02	0.05 ± 0.02
<i>B. cereus</i> MTCC 430	12.46 ± 0.50	0.01 ± 0.00	0.04 ± 0.00	0.20 ± 0.25	0.10 ± 0.08

CONCLUSION

The current research work is an endeavor to biologically synthesize silver nanoparticles using the callus of *C. roseus* under controlled conditions. This callus based route also provides the availability of sample material throughout the year. Also critically endangered and medicinally prominent plant species is used. The growth and development of callus is greatly affected by changes in photoperiod and pH observed via

two different experiments. The callus was exposed to different photoperiods : Controlled, SD and LD and kept under observation for 7 and 14 days respectively. Induction and growth of callus and its pigmentation were found to be greatest at Controlled condition. Growth and development of callus showed a negative trend for SD and LD. Secondary metabolism processes are directly influenced by change in photoperiod and pH.

In another experiment, callus was observed at pH 5.0, 6.5 and 7.0. At pH 5.7, the best callus development and its pigmentations were observed while at other pH, callus growth was very slow and callus was of distorted morphology.

Silver nanoparticles from controlled-CME at 7 and 14 days and at pH 5.7 demonstrated highest antimicrobial activity (in synergy with streptomycin) against all six pathogens at 200µg/ml concentration. No antibacterial activity was obtained in SD and LD condition of 7 and 14 days duration and also for different pH 5.0, 6.5, and 7.0.

TEM analysis showed an average size of 19.13 nm of AgNPs. Spherical uniform shape in AgNPs was achieved only under controlled light conditions. The phytochemicals present in the callus extract contains different functional groups which are confirmed by FTIR analysis. The phase composition and purity of the synthesized AgNPs is revealed by XRD patterns whereas metal composition is determined by EDX results. Uniform distribution is confirmed by DLS method.

Future prospects

The mass scale production of nanoparticles can be a realistic future due to successful, feasible and eco-friendly synthesis of nanoparticles as confirmed by the results of this study. Moreover, synthesis of metal nanoparticles by using callus extract under controlled light conditions will be a benefiting factor as it renders regulation of size and shape of NPs in order to develop nanoparticles of varied attributes which shall possess multiple advantages across several commercial industries.

These CME synthesized nanoparticles have attracted attention of scientists, researchers as well as industrialists worldwide due to their competence for use in diversified fields like therapeutics, pharmaceuticals industry including cancer treatment drug, drug carriers, biomolecular detection, agriculture due to the presence of secondary metabolites and antioxidants and variety of commercial uses as biosensors, cosmetics, catalysts, medical textiles, nano-electronics, UV protection systems etc. Green-synthesized AgNPs may be further explored and develop as a capable antibacterial agent for a vast variety of infectious microorganisms. This will also attract development of newer compounds to fight against multi-drug resistant bacteria and reduce the dependency on synthetic drugs.

AUTHOR CONTRIBUTION

MG performed all the experiments and wrote the manuscript draft and design the concept and finalized the manuscript.

CONFLICT OF INTERESTS

The authors confirm they have no conflict of interests.

DATA AVAILABILITY STATEMENT IN YOUR MANUSCRIPT

All the raw data available

FUNDING STATEMENT

No funding available. AUMP Gwalior provided the money for research work.

ACKNOWLEDGEMENT

We wish to express our sincere acknowledgement to Dr. Ashok Kumar Chauhan, President, RBEF parent organization of Amity University Madhya Pradesh (AUMP), Dr. Aseem Chauhan, Additional President, RBEF and chairman of Amity University Gwalior Campus, Lt. Gen. V.K. Sharma, AVSM (Retd.), Vice Chancellor of AUMP Gwalior Campus, for providing necessary facilities, their valuable support and encouragement throughout the work.

REFERENCES

1. Calderón-Jiménez B, Johnson ME, Montoro Bustos AR, Murphy KE, Winchester MR, Vega Baudrit JR. (2017). Silver nanoparticles: technological advances, societal impacts, and metrological challenges. *Frontiers in chemistry*, 5:6. doi: 10.3389/fchem.2017.00006.
2. Lee SH, Jun BH. (2019). Silver Nanoparticles: Synthesis and application for nanomedicine. *Int. j of mol. sci.*, 20(4):865. doi: 10.3390/ijms20040865.

3. Agnihotri S, Mukherji S, Mukherji S. (2014). Size-controlled silver nanoparticles synthesized over the range 5–100 nm using the same protocol and their antibacterial efficacy. *Rsc Adv.*, 4(8):3974-83. <https://doi.org/10.1039/C3RA44507K>.
4. Mourdikoudis S, Pallares RM, Thanh NT. (2018). Characterization techniques for nanoparticles: Comparison and complementarity upon studying nanoparticle properties. *Nanoscale*, 10(27):12871-12934. <https://doi.org/10.1039/C8NR02278J>.
5. Gurunathan S, Han JW, Kim ES, Park JH, Kim JH. (2015). Reduction of graphene oxide by resveratrol: A novel and simple biological method for the synthesis of an effective anticancer nanotherapeutic molecule. *Int. j. of nanomedicine*, 10:2951. <https://doi.org/10.2147/IJN.S79879>.
6. Sapsford KE, Tyner KM, Dair BJ, Deschamps JR, Medintz IL. (2011). Analyzing nanomaterial bioconjugates: a review of current and emerging purification and characterization techniques. *Analytical chemistry*, 83(12) : 4453-4488. doi: 10.1021/ac200853a.
7. Runa R and Trivedi MP. (2015). Rapid *In-Vitro* Regeneration of an Important Medicinal and an Ornamental Plant (*Catharanthus roseus* L). *Biochem Anal Biochem.*, 4:227. DOI :10.4172/2161-1009.1000227
8. da Silva JA, Winarto B, Dobránszki J, Zeng S. (2015). Disinfection procedures for in vitro propagation of Anthurium. *Folia Horticulturae*, 27(1):3-14. DOI: <https://doi.org/10.1515/fhort-2015-0009>.
9. Thomas TD, and Shankar S. (2009). Multiple shoot induction and callus regeneration in *Sarcostemma brevistigma* Wight & Arnott, a rare medicinal plant. *Plant Biotech. Reports*, 3(1): 67. DOI: 10.1007/s11816-008-0076-1.
10. Prakash MB, Paul S. (2012). Green synthesis of silver nanoparticles using *Vinca roseus* leaf extract and evaluation of their antimicrobial activities. *Int J Appl Biol Pharma Technol.*, 3(4):105–111. doi: 10.1016/j.colsurfb.2013.03.017.
11. Ponarulselvam S, Panneerselvam C, Murugan K, Aarthi N, Kalimuthu K, Thangamani S. (2012). Synthesis of silver nanoparticles using leaves of *Catharanthus roseus* Linn. G. Don and their antiplasmodial activities. *Asian Pacific j. of tropical biome.*, 2(7): 574-580. [https://doi.org/10.1016/S2221-1691\(12\)60100-2](https://doi.org/10.1016/S2221-1691(12)60100-2).
12. Gupta M, Tomar RS, Mishra RK. (2020). Factors affecting biosynthesis of green nanoparticles. *Our Heritage*, 11-22.
13. Mukhri Z, Yamaguchi H. (1986). In vitro plant multiplication from rhizomes of turmeric (*Curcuma domestica* Val.) and temoe lawak (*C. xanthoriza* Roxb.). *Plant tissue culture let.*, 3(1): 28-30. DOI:10.5511/PLANTBIOTECHNOLOGY1984.3.28.
14. Kim J, Rheem Y, Yoo B, Chong Y, Bozhilov KN, Kim D, Sadowsky MJ, Hur HG, Myung NV. (2010). Peptide-mediated shape- and size-tunable synthesis of gold nanostructures. *Acta Biomaterialia.*, 6(7):2681-9. [10.1016/j.actbio.2010.01.019](https://doi.org/10.1016/j.actbio.2010.01.019).
15. Saber MM, Mirtajani SB, Karimzadeh K. (2018). Green synthesis of silver nanoparticles using *Trapa natans* extract and their anticancer activity against A431 human skin cancer cells. *Journal of Drug Delivery Science and Tech.*, 47: 375-379. <https://doi.org/10.1371/journal.pone.0216496>
16. Chattopadhyay RR, Sarkar SK, Ganguly S, Medda C, Basu TK. Hepatoprotective activity of *Ocimum sanctum* leaf extract against paracetamol included hepatic damage in rats. *Indian J Pharmacol Heptato*, 1992, 24: 163-5.
17. Ahmad N, Sharma S. (2012). Green synthesis of silver nanoparticles using extracts of *Ananas comosus*. *Green and Sustainable Chemistry*, 2(04): 141. DOI: 10.4236/gsc.2012.24020.
18. Ahmad N, Rab A, Ahmad N. (2016). Light-induced biochemical variations in secondary metabolite production and antioxidant activity in callus cultures of *Stevia rebaudiana* (Bert). *Journal of Photochemistry and Photobiology B: Biology*, 154:51-6. doi: 10.1016/j.jphotobiol.2015.11.015.
19. Kim MJ, Kim SH, Park HY, Huh YD. (2011). Morphological evolution of Ag 2 O microstructures from cubes to octapods and their antibacterial activities. *Bulletin of the Korean Chemical Soci.*, 32(10):3793-5. <https://doi.org/10.5012/bkcs.2011.32.10.3793>.
20. Trivedi M, Tallapragada RM, Branton A, Trivedi D, Nayak G, Latiyal O, Jana S. (2015). The potential impact of biofield energy treatment on the physical and thermal properties of silver oxide powder. *Int. J. of Biomed. Sci. and Eng.*, 5(3): 62-68. doi: 10.11648/j.ijbse.20150305.11.
21. Ramos-Escudero F, Muñoz AM, Alvarado-Ortíz C, Alvarado A, Yáñez JA. (2012). Purple corn (*Zea mays* L.) phenolic compounds profile and its assessment as an agent against oxidative stress in isolated mouse organs. *J. of medicinal Food.*, 15(2): 206-215. doi: 10.1089/jmf.2010.0342.
22. Bacchetti T, Masciangelo S, Micheletti A, Ferretti G. (2013). Carotenoids, phenolic compounds and antioxidant capacity of five local Italian corn (*Zea mays* L.) kernels. *Journal of Nutrition & Food Sci.*, 3(6):1. DOI: 10.4172/2155-9600.1000237.
23. Pandey R, Singh A, Maurya S, Singh U P, Singh M. (2013). Phenolic acids in different preparations of Maize (*Zea mays*) and their role in human health. *Int. J. Curr. Microbiol. App. Sci.*, 2(6): 84-92.
24. Makarov VV, Love AJ, Sinitsyna OV, Makarova SS, Yaminsky IV, Taliansky ME, Kalinina NO. (2012). Green nanotechnologies: synthesis of metal nanoparticles using plants. *Acta Naturae*, 6:1-20.
25. Glusker PJ, Katz KA, Bock CW. (1999). Metal ions in biological systems. *Rigaku J.*, 16(2): 8-17. DOI:10.1201/9781482289893.
26. Si S, and Mandal TK. Tryptophan-based peptides to synthesize gold and silver nanoparticles: A mechanistic and kinetic study. *Chemistry–A European J.*, 2007, 13(11): 3160-3168. <https://doi.org/10.1002/chem.200601492>.
27. Glusker PJ, Katz KA, Bock CW. Metal ions in biological systems. *Rigaku J.*, 1999, 16(2): 8–16.
28. Noth MH, Abel WO. (1971). For the development of haploid plants from immature microspores of various *Nicotiana* species. *Z. plant breeding*, 65:277-284.

29. Morris P. (1986). Regulation of product synthesis in cell cultures of *Catharanthus roseus*. Effect of culture temperature. Plant cell reports, 5(6): 427-429. doi: 10.1007/BF00269633.
30. Seibert M, and Kadkade PG. (1980). Environmental factors. A. Light. Plant tissue culture as a source of biochemicals, 123-141.
31. Cornejo-Martin MJ, Mingo-Castel AM, Primo-Millo E.(1979). Organ redifferentiation in rice callus: effects of C₂H₄, CO₂ and cytokinins. Zeitschrift für Pflanzenphysiologie, 94(2):117-23.
32. Sunderland N. Anther culture: a progress report. Science Progress, 1971, 1933: 527-549.
33. Beveridge TJ. (1999). Structures of gram-negative cell walls and their derived membrane vesicles. Journal of bacteriology, 181(16):4725-33. DOI: 10.1128/JB.181.16.4725-4733.1999

CITATION OF THIS ARTICLE

Monika Gupta. Production of silver nanoparticles from *Catharanthus roseus* under controlled physiological environment: A pioneer advancement to combat antibiotic-resistant microbes. Bull. Env. Pharmacol. Life Sci., Vol10[3] February 2021 : 92-108